表 1 疾患別の初診時・最終観察時所見

症例	性別	患側	初診時年齢（か月）	合併症（眼以外）	眼圧（mmHg）	角膜径（垂直 mm×水平 mm）	前医からの抗緑内障点眼薬（剤）	経過観察時 最高眼圧（mmHg）	最終観察時所見 眼圧（mmHg）	緑内障手術回数（回）	緑内障点眼薬（剤）	経過観察期間（か月）
Peters 奇形												
1	女	右	4	水腎症，心房中隔欠損症	Tn+1	13.5×13.5	1	30[i]	30[g]	2	0	80
		左			Tn	14.0×13.0	1	30[i]	30[g]	0	2	
2	女	右	2	なし	19[i]	6.0×7.0	0	19[i]	Tn	0	0	13
		左			23[i]	6.0×7.0	0	23[i]	Tn	0	0	
3	男	右	3	なし	34[p]	11.0×10.5	2*	34[p]	10[i]	0	2	10
		左			34[p]	14.0×15.5	2*	34[p]	11[i]	1	2	
4	女	左	3	なし	25[p]	10.0×16.0	2*	25[p]	10[i]	0	1	10
5	男	右	4	なし	Tn	NA	1	18[i]	10[i]	0	1	9
		左			Tn	NA	1	16[i]	6[i]	0	1	
6	女	右	4	なし	Tn	NA	0	16[i]	測不	0	0	7
		左			Tn	NA	0	12[i]	測不	0	0	
7	女	右	1	多発奇形[注1]	Tn+2	NA	3	18[t]	14[p]	1	3	2
		左			Tn+2	NA	3	26[t]	19[p]	1	3	
強膜化角膜												
8	女	右	8	なし	Tn	測不	0	35[n]	測不	0	0	88
		左			Tn	測不	0	26[n]	16[n]	0	1[注3]	
9	女	右	47	多発奇形[注2]	Tn	測不	0	23[i]	16[i]	0	0	14
		左			Tn	測不	0	30[i]	22[i]	0	0	
10	女	右	2	精神発達遅延，足指癒着	Tn	測不	0	33[i]	16[i]	0	1	38
		左			Tn	測不	0	17[i]	15[i]	0	1	

*：合剤1剤使用のため2剤として換算，g：Goldmann 圧平眼圧計，n：ノンコンタクトトノメーター，p：Perkins 圧平眼圧計，i：iCare®，t：TONO-PEN®

注1）：動脈管開存症，脳梁発育不全，右膀胱尿管逆流症，左多嚢胞腎．

注2）：喉頭軟化症，脳梁欠損，心房中隔欠損症，てんかん，染色体異常（21モノソミー）．

注3）：抗緑内障点眼薬が開始されているのは角膜移植後の眼圧上昇のためであり，発達緑内障のためではない．

グレーの網掛け：発達緑内障．

NA：カルテ記載なし，測不：測定不能．

から角膜にかけての境界を同定できず，角膜全体が混濁しているものを強膜化角膜と判断した（図1）．

また，通常，角膜混濁のない発達緑内障の合併については，眼圧，視神経乳頭の形状，角膜径の拡大傾向，角膜浮腫の有無などから判断されるが[5)13)]，先天角膜混濁の症例では眼底の観察ができず，角膜径の拡大傾向と眼圧値が重要な情報となる．小児では成長とともに角膜径は増大し，新生児の角膜径はおおよそ9.5～10.5 mmであり，生後2年頃までに10.8～11.5 mmに増加すると報告されている[14)15)]．今回，我々が検討を行った先天角膜混濁の症例は，全例において眼底の観察が不可能で視神経乳頭の形状が確認できなかった．そこで，眼圧の推移，緑内障点眼薬の有無，角膜径の拡大傾向の有無などを総合的に判断して緑内障を診断した．

全症例でUBM（トーメーコーポレーション社製，UD-6000UBM）を用いて，Descemet膜欠損，虹彩からの索状物の立ち上がり，虹彩前癒着，部分的隅角閉塞，無虹彩，前房深度，前房隅角異常の有無を判定し，前眼部所見，眼圧，臨床経過とUBM所見との関係を比較，検討した．得られた結果の数値記載については，すべて平均値±標準偏差で記載した．

Ⅲ 結 果

全例（10例19眼）が他院からの紹介患者であった．Peters奇形は男児2例4眼，女児5例9眼，初診時の平均年齢は3.0±1.2か月，平均経過観察期間18.7±27.2か月であった．強膜化角膜は男児0例，女児3例6眼，初診時の平均年齢19.0±24.4か月，経過観察期間46.7±37.8か月であった．Peters奇形7例中の6例が両眼性であり，強膜化角膜は全例が両眼性であった．

Peters奇形の初診時の眼圧はPerkins圧平眼圧計またはiCare®にて測定可能であった3例5眼では平均眼圧が27.0±6.7 mmHgとやや高値であり，測定不可であった4例のうち触診Tnが3例5眼，Tn+1が1例1眼，Tn+2が1例2眼であった．一方，強膜化角膜の3例6眼は初診時に眼圧を測定できず，触診にてすべて

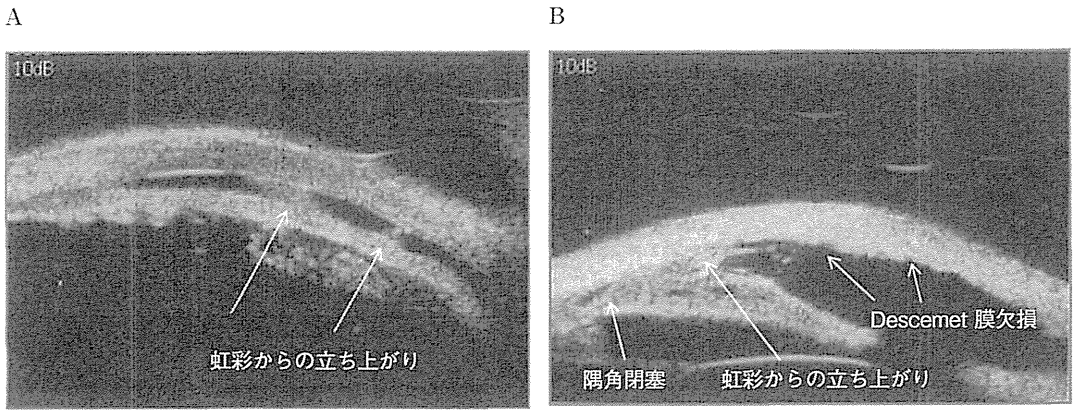

図 2　超音波生体顕微鏡(UBM)所見.
A：Peters 奇形(症例 6)では，虹彩から角膜後面に向かう索状物の立ち上がりを認める.
B：強膜化角膜(症例 10)では，隅角閉塞，虹彩から角膜後面に向かう索状物の立ち上がり，Descemet 膜欠損を認める.

Tn と判断された．角膜径の拡大傾向を伴った症例を緑内障に分類すると，緑内障の合併が Peters 奇形で 5 例 9 眼(69.2%)にみられたのに対して，強膜化角膜では 1 例 2 眼(33.3%)であった(表 1)．これらの緑内障合併例では初診時に紹介元ですでに緑内障の診断がされていた．緑内障合併の Peters 奇形は，当院受診前より緑内障点眼薬が使用されていた(表 1 の症例 1，3〜5，7)．一方，緑内障合併の強膜化角膜は点眼なしの状態で紹介され，当院経過観察中に緑内障点眼薬を開始した(表 1 の症例 10)．

Peters 奇形の UBM 所見は，前房深度が 1.40±0.84 (range 0.30〜2.40) mm，中心角膜厚が 0.63±0.32 (0.46〜0.77)mm，であり，特徴として，角膜中央部を中心とした Descemet 膜欠損，虹彩から角膜内皮面に向けての索状物の立ち上がり，虹彩前癒着，部分的隅角閉塞が顕著にみられた(図 2，表 2)．一方，強膜化角膜の UMB 所見は，前房深度が 1.89±1.02 (1.52〜2.33) mm，中心角膜厚が 0.83±0.46 (0.64〜1.14) mm であり，Peters 奇形と同様に，角膜中央部を中心とした部分的 Descemet 膜欠損，虹彩から角膜内皮面に向けての索状物の立ち上がり，虹彩前癒着，部分的隅角閉塞を認めた(図 2，表 2)．

Peters 奇形は強膜化角膜に比べて緑内障合併率が高かったにもかかわらず，UBM 所見において両者の隅角所見に明らかな違いを認めなかった．

Ⅳ　考　　按

今回の検討では全体の 57.9% に緑内障の合併を認めた．病型別では，Peters 奇形 7 例 13 眼中，5 例 9 眼(69.2%)，強膜化角膜 3 例 6 眼中，1 例 2 眼(33.3%)と，Peters 奇形の半数において緑内障の合併を認めた．海外の報告によると Peters 奇形の緑内障合併率は 50%〜70% であり[1)〜8)]，当院での検討結果も過去の報告と類似であった．先天角膜混濁では白濁した角膜を主訴に受診されることが多く，眼圧を測定せずに紹介される例もあるが，常に眼圧上昇や角膜径の拡大について注意が必要である．強膜化角膜 3 例のうち 1 例で角膜径の拡大傾向を認めたため緑内障を疑い，抗緑内障薬を開始したが，本症例は精神発達遅延があり常に指で両眼を押す動作がみられたため，その影響を否定できない．

UBM 所見は全症例で Descemet 膜欠損，虹彩前癒着を認め，Peters 奇形 1 例 1 眼を除いた 9 例 18 眼で虹彩から立ち上がる索状物を認めた．部分的隅角閉塞は Peters 奇形の 5 例 10 眼，強膜化角膜の 3 例 5 眼で認められた．Peters 奇形と強膜化角膜との間に特に明らかな違いが見出せなかったことより，今回の症例においては UBM 所見からの病型の診断は難しいと考える．

UBM で測定した前房深度は Peters 奇形，強膜化角膜ともに，既報にある正常な小児の前房深度[16)17)]と比較して浅い結果であった．ただし，浅前房を伴う 6 眼(表 2 の症例 3 右，4 左，6 右左，7 右，9 左)のうち，緑内障と診断された症例は 3 眼(表 1 の症例 3 右，4 左，7 右)であった．緑内障の合併の有無と UBM 所見に関連を認めず，UBM では検出できない隅角の機能異常により眼圧上昇を来すことが推測された．

正常乳幼児の角膜厚の平均は測定対象の人種や測定条件などの違いにより異なり[18)〜20)]，本邦では山本ら[21)]が正常乳幼児の角膜厚の平均を報告している(0 歳：0.488 mm，1 歳：0.510 mm，2 歳：0.515 mm，3 歳：0.529 mm，4 歳：0.521 mm)．今回，角膜厚を測定できた Peters 奇形 5 例 9 眼，強膜化角膜 2 例 4 眼のうち Peters 奇形は 6 眼で 0.6 mm を超え，強膜化角膜は 4 眼で 0.6 mm を超えていた．そこで，これらの中心角膜厚が眼圧に影響している可能性を考え，Suzuki ら[22)]の眼圧補正式〔補正眼圧値＝測定眼圧値－0.012(中心角膜厚＜μm＞－520)〕で今回得られた眼圧を補正してみたが，初診時角

表 2 疾患別 UBM 所見

症例	性別	患側	Descemet 膜欠損	虹彩からの索状物の立ち上がり	虹彩前癒着	部分的隅角閉塞	無虹彩	浅前房	中心角膜厚(mm)	前房深度(mm)
Peters 奇形										
1	女	右	+	+	+	+	+	−	測不	測不
		左	+	+	+	+	+	−	測不	測不
2	女	右	+	+	+	+	−	−	0.77	1.61
		左	+	+	+	+	−	−	0.73	1.84
3	男	右	+	+	+	−	−	+	0.53	1.21
		左	+	+	+	−	+	−	0.62	1.45
4	女	左	+	−	+	−	−	+	0.48	1.39
5	男	右	+	+	+	+	−	−	0.46	2.40
		左	+	+	+	+	−	−	0.64	1.67
6	女	右	+	+	+	+	−	+	0.70	0.30
		左	+	+	+	+	−	+	0.72	0.74
7	女	右	+	+	+	+	−	+	測不	測不
		左	+	+	+	+	−	−	測不	測不
所見の該当率(%)			100(13/13)	92(12/13)	100(13/13)	77(10/13)	23(3/13)	38(5/13)		
強膜化角膜										
8	女	右	+	+	+	+	−	−	測不	測不
		左	+	+	+	+	−	−	測不	測不
9	女	右	+	+	+	−	−	−	1.14	2.33
		左	+	+	+	+	−	+	0.84	1.70
10	女	右	+	+	+	+	−	−	0.64	2.02
		左	+	+	+	+	−	−	0.70	1.52
所見の該当率(%)			100(6/6)	100(6/6)	100(6/6)	83(5/6)	0(0/6)	17(1/6)		

測不：測定不能.

膜厚を考慮しても眼圧は高かった.

今回検討した症例の中には，初診時眼圧は正常範囲であっても，経過中に眼圧が上昇し角膜径が拡大傾向となったために，検討期間を過ぎてから点眼が開始される症例があった(症例 9)．眼圧が上昇傾向にある場合，角膜径の拡大傾向が生理的な成長を上回る場合などは，こまめに診察をしていくことが重要である．角膜混濁の程度，眼圧，角膜径(垂直，水平)，観察できる場合には視神経乳頭陥凹比の推移を記録し，角膜混濁の程度については写真などでも記録，追跡することが望ましい.

Nischal ら[10]は先天角膜混濁 13 例 22 眼について臨床診断，UBM 所見，移植した 13 眼の病理所見を比較，検討し，5 眼において UBM 後に臨床診断を変更，UBM 所見と病理所見が一致することを報告した．今回検討した 10 例のうち，移植を行ったのは症例 8 のみであり，臨床診断と病理所見は強膜化角膜で合致した[23]．しかし症例 8 は他院で Peters 奇形の診断を受けており，両疾患の鑑別は難しいといえる.

今回，小児先天角膜混濁症例の眼圧，臨床所見と UBM 所見の検討を行った．UBM 所見により，Peters 奇形と強膜化角膜の前房隅角形状の類似性が判明した．Peters 奇形は強膜化角膜よりも緑内障合併率が高かったが，緑内障合併の有無による UBM 所見の相違を認めなかった．先天角膜混濁における隅角の機能異常については，さらなる検討を要する.

利益相反：利益相反公表基準に該当なし

文 献

1) **Bermejo E, Martínez-Frías ML**：Congenital eye malformations：clinical-epidemiological analysis of 1,124,654 consecutive births in Spain. Am J Med Genet 75：497-504, 1998.
2) **Ciralsky J, Colby K**：Congenital corneal opacities：a review with a focus on genetics. Semin Ophthalmol 22：241-246, 2007.
3) **Kenyon KR**：Mesenchymal dysgenesis in Peters' anomaly, sclerocornea and congenital endothelial dystrophy. Exp Eye Res 21：125-142, 1975.
4) **Rezende RA, Uchoa UB, Uchoa R, Rapuano CJ, Laibson PR, Cohen EJ**：Congenital corneal opacities in a cornea referral practice. Cornea 23：565-570, 2004.
5) **Rubin SE, Marcus CH**：GLAUCOMA IN CHILD-

HOOD. Ophthalmol Clin North Am 9：215-227, 1996.
6) **Yang LL, Lambert SR**：Peters' anomaly. A synopsis of surgical management and visual outcome. Ophthalmol Clin North Am 14：467-477, 2001.
7) **Stone DL, Kenyon KR, Green WR, Ryan SJ**：Congenital central corneal leukoma (Peters' anomaly). Am J Ophthalmol 81：173-193, 1976.
8) **Basdekidou C, Dureau P, Edelson C, De Laage De Meux P, Caputo G**：Should unilateral congenital corneal opacities in Peters' anomaly be grafted? Eur J Ophthalmol 21：695-699, 2011.
9) **Shigeyasu C, Yamada M, Mizuno Y, Yokoi T, Nishina S, Azuma N**：Clinical features of anterior segment dysgenesis associated with congenital corneal opacities. Cornea 31：293-298, 2012.
10) **Nischal KK, Naor J, Jay V, MacKeen LD, Rootman DS**：Clinicopathological correlation of congenital corneal opacification using ultrasound biomicroscopy. Br J Ophthalmol 86：62-69, 2002.
11) **國原依里子，竹中丈二，近間泰一郎，木内良明**：前眼部の形態変化を観察できた前眼部形成不全の1例．日眼会誌 116：650-656, 2012.
12) **朴　真紗美，桐生純一，栗本康夫，小林　博，近藤武久**：超音波バイオマイクロスコープによる強膜化角膜と小角膜の前眼部の観察．日眼会誌 101：69-73, 1997.
13) **Tamçelik N, Atalay E, Bolukbasi S, Çapar O, Ozkok A**：Demographic features of subjects with congenital glaucoma. Indian J Ophthalmol 62：565-569, 2014.
14) **塚原康友，山本　節**：正常小児角膜内皮の生後発達．日眼会誌 93：763-768, 1989.
15) **Kiskis AA, Markowitz SN, Morin JD**：Corneal diameter and axial length in congenital glaucoma. Can J Ophthalmol 20：93-97, 1985.
16) **Blomdahl S**：Ultrasonic measurements of the eye in the newborn infant. Acta Ophthalmol (Copenh) 57：1048-1056, 1979.
17) **Kobayashi H, Ono H, Kiryu J, Kobayashi K, Kondo T**：Ultrasound biomicroscopic measurement of development of anterior chamber angle. Br J Ophthalmol 83：559-562, 1999.
18) **Rushood AA, Zahrani MH, Khamis A, Rushood AA**：Central corneal thickness in full-term Saudi newborns. Acta Ophthalmol 90：e355-358, 2012.
19) **Portellinha W, Belfort R Jr**：Central and peripheral corneal thickness in newborns. Acta Ophthalmol (Copenh) 69：247-250, 1991.
20) **Remón L, Cristóbal JA, Castillo J, Palomar T, Palomar A, Pérez J**：Central and peripheral corneal thickness in full-term newborns by ultrasonic pachymetry. Invest Ophthalmol Vis Sci 33：3080-3083, 1992.
21) **山本　節，西崎雅也**：乳幼児における角膜厚と眼圧について．眼臨紀 1：349-351, 2008.
22) **Suzuki S, Suzuki Y, Iwase A, Araie M**：Corneal thickness in an ophthalmologically normal Japanese population. Ophthalmology 112：1327-1336, 2005.
23) **Young RD, Quantock AJ, Sotozono C, Koizumi N, Kinoshita S**：Sulphation patterns of keratan sulphate proteoglycan in sclerocornea resemble cornea rather than sclera. Br J Ophthalmol 90：391-393, 2006.

白内障・屈折手術の論点

緑内障と白内障同時手術派

京都府立医大　日野　智之，森　和彦

1．はじめに

緑内障の治療において，点眼のみでは目標眼圧まで下降できない場合，あるいは早急な眼圧下降が望ましい場合などに，緑内障手術を検討する必要がある。その際に，白内障手術の適応があった場合に，緑内障手術を単独で行い眼圧コントロールをした後に二期的に白内障手術を行うか，白内障手術を単独で行い二期的に緑内障手術を行うか，あるいは，緑内障と白内障を同時に手術するかの選択をする必要がある。どの選択が最善であるかは症例ごとで状況が異なるため，最終的には術者の判断になる。今回，ここでは，緑内障と白内障を同時に行うことの利点について述べたいと思う。

緑内障と白内障を同時に手術することの最大の利点は，手術が一度ですむ点である。近年，高齢化が進み，手術を必要とする患者も高齢化している。緑内障以外にも身体に疾患を抱える患者も多く，二度に分けて手術を受ける患者の身体的・精神的負担は大きい。また，家族などの患者を支える周辺の方への負担も大きなものとなる。一度に手術をすることで，それらの負担を軽減することが可能である。

手術を同時に実施することで，身体はもちろんのこと，眼への負担も軽減される。最近では手術機械の進歩も著しく，より低侵襲での手術も可能であるが，内眼手術を行う以上は，角膜内皮細胞減少が不可避である。角膜内皮細胞減少により水疱性角膜症に至ることは周知のとおりである。緑内障手術が必要な症例のなかには，偽落屑症候群のように角膜内皮細胞減少に関与する疾患もあり，術前から角膜内皮細胞が少ない症例も多々ある。また，緑内障手術は複数回の手術が必要になる症例も多い。これらのことからも，同時に行える症例であれば同時手術が望ましいと考える。

白内障手術と同時に行う緑内障手術として，線維柱帯切除術（trabeculectomy 以下 TLE），線維柱帯切開術（trabeculotomy 以下 TLO），隅角癒着解離術（goniosynechialysis 以下 GSL）が現在行われている主な手術である。それぞれの手術について，白内障手術と同時に行うことに関して考察する。

2．術　式

2．1．TLE併用白内障手術

TLEが必要な症例では，TLEを単独で施行した後に白内障手術を行うか，白内障手術を施行した後にTLEを行うかの二期的に行うか，TLE併用白内障手術（図1）を施行するかの選択をする必要がある。ここでは，一般的に白内障を有し，同時手術の適応がある症例で，TLE併用白内障手術を選択する利点を述べたいと思う。

緑内障手術が必要な症例では，手術の第一の目的は眼圧下降である。TLE単独で手術を行った場合と，TLE併用白内障手術を行った場合の眼圧下降に関しては様々な報告がある。El-Sayyadら[1]は，TLE後に

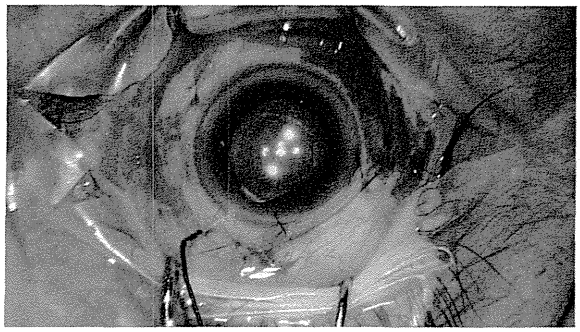

図1　線維柱帯切除術（TLE）併用白内障手術の術中写真

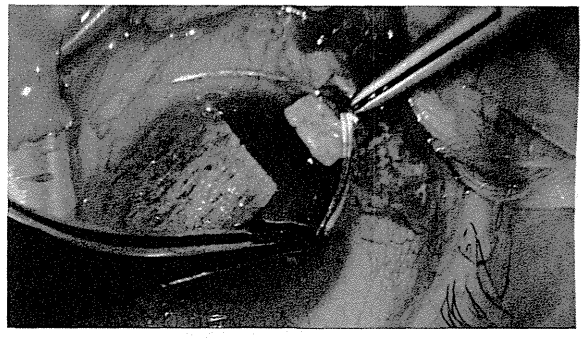

図2　線維柱帯切開術（TLO）併用白内障手術の術中写真
トラベクロトームをシュレム管に挿入し回転させている。

白内障手術を行った群と，TLEと白内障手術を同時に行った群では術後半年，1年後の眼圧下降はほぼ同等であり，良好な下降が得られたと報告している。黒田[2]は，同時手術の眼圧コントロールは単独手術と同等であったと報告している。

TLE後に二期的に白内障手術を行うと，濾過胞が縮小または消失し，眼圧コントロールも悪くなると考えられてきた。狩野ら[3]は，角膜小切開によるPEAであっても，術後の濾過胞縮小による眼圧レベルの上昇のリスクが高いと報告している。現在では小切開超音波白内障手術が主流になり，マイトマイシンCの使用などにより同時手術の成績も向上しており，二期的に手術を行うよりは同時手術を選択した方が望ましいと考える。

これまで，原発閉塞隅角緑内障（primary angle-closure glaucoma 以下 PACG）に対するTLEは併発症の頻度が高く，とくに急性閉塞隅角緑内障発作後の症例に対するTLEは，駆逐性出血，過剰濾過に伴う浅前房と，それに伴う角膜内皮障害，低眼圧，脈絡膜剝離の遷延による黄斑症，毛様体－水晶体ブロックによる悪性緑内障などの重篤な合併症が起こりやすいと報告[4]されてきた。鈴木ら[5]は，PACGに対するTLE併用白内障手術は，眼圧下降効果が大きく，積極的な眼圧下降治療が必要な症例に有用であったと報告している。

TLEの適応となる疾患は多く存在する。年齢，白内障の程度など個々の症例で状況が異なるため，TLEが必要な症例で同時に白内障手術を施行するかどうかの最終判断は主治医に委ねられることはもちろんであるが，白内障と同時に実施することの利点は多く，積極的に考慮するべきであると考える。

2. 2. TLO併用白内障手術

TLOを施行する際に，白内障手術が適用である場合には，TLE同様に白内障手術と同時にTLOを行う（図2）か，白内障術後にTLO，TLO術後に白内障手術を行うかの選択をする必要がある。TLOはSchlemm管内壁を開放する手術で濾過胞を作らないため，TLEのように濾過胞にかかわる合併症や，留意点は考慮する必要はない。松村ら[6]は，白内障手術とTLOを同時に行った20眼と，TLOを先に行い後から白内障手術を行った29眼と，白内障手術を行い後にTLOを行った4眼の，術後24カ月での平均眼圧に有意差を認めなかったと報告している。同時手術，単独手術で眼圧下降に差がないのであれば，上述した患者の負担や，単独手術後に再度手術を受ける必要が出てくる可能性などを踏まえれば，白内障手術適用のTLO手術時には，TLO併用白内障手術が第一選択であると考える。

2. 3. GSL併用白内障手術

緑内障診療ガイドライン第3版では，GSLの適応となる疾患としてPACG，続発閉塞隅角緑内障が挙げられている。

隅角閉塞機序は，以下の因子が関与していると考えられている。

1）相対的瞳孔ブロック：瞳孔領における虹彩－水晶体間の房水の流出抵抗の上昇に引き続く虹彩の前方膨隆により隅角閉塞を来す。
2）プラトー虹彩：虹彩根部が前方に屈曲し，散瞳時に直接隅角を閉塞する虹彩の形態異常である。

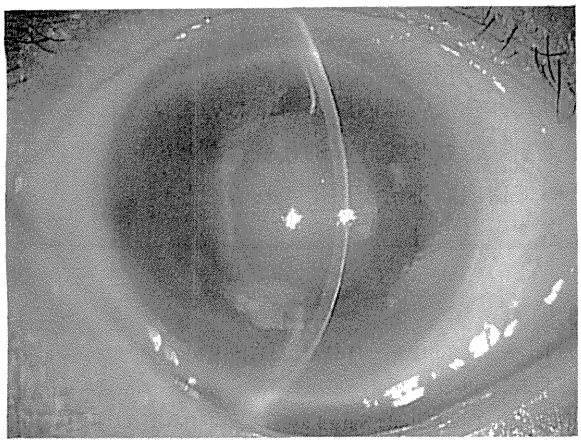

図3　急性緑内障発作の症例
角膜浮腫，浅前房，瞳孔ブロックの所見がみられる。

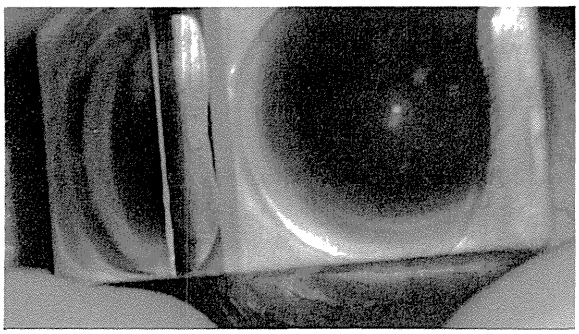

図4　図3症例に対する隅角癒着解離術（GSL）併用白内障手術の術中写真①
森ゴニオレンズ㊞を用いて隅角を観察している。

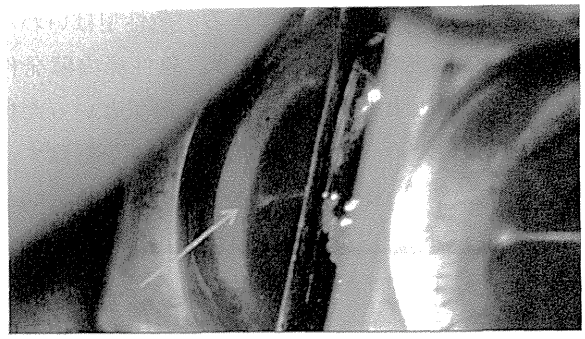

図5　図3症例に対するGSL併用白内障手術の術中写真②
隅角癒着解離針で隅角の癒着を解離している（矢印）。

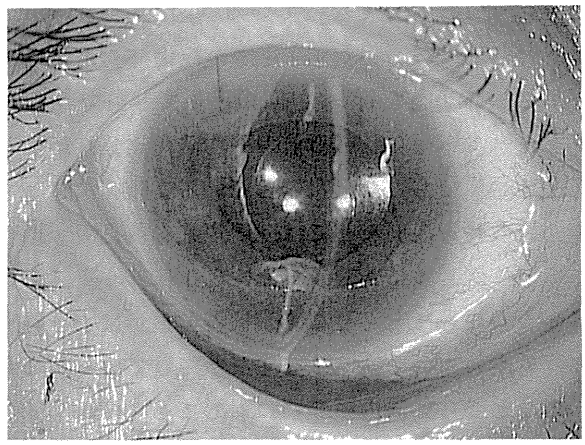

図6　図3症例に対するGSL併用白内障手術後の前眼部写真
前房は深くなり，眼圧も下降し，術後経過は良好である。

3）水晶体因子：水晶体の前進，膨隆，加齢による増大も原発性の隅角閉塞発症に関与している。

4）毛様体因子：画像診断においてのみ診断可能な微小な特発性の毛様体脈絡膜滲出を伴う原発閉塞隅角症/緑内障の症例が存在し，浅前房化，毛様体ブロックの増強による閉塞隅角に関与することが推測されている。

これらの因子のなかで，1）相対的瞳孔ブロック，2）プラトー虹彩，3）水晶体因子が関与する場合の手術加療として，隅角閉塞の直接の要因である水晶体を摘出することと，GSLにより隅角を開大させることを同時に行うことは理にかなった加療であると考える。有水晶体眼におけるGSL単独手術は長期的にみると眼圧コントロールに不安があり，水晶体摘出が避けられない症例も存在する。河野[7]は，PACG36例38眼に対するGSLの成績について，GSL単独手術（11眼）の初回コントロール率は45.5％であったが，GSL併用白内障手術（21眼）の初回コントロール群は90.5％であった。また，GSL単独手術を行った11眼のうち3眼は再手術で水晶体を摘出したと報告している。GSL単独手術を行う場合，透明水晶体であることや，調節力の維持ということを考慮され水晶体を温存するという選択をしている場合が多い。しかし，GSL単独手術による侵襲や，他要素により白内障の進行は想定されることや，水晶体が閉塞隅角の要因の一つであることなども考えれば，GSL単独手術よりもGSL併用白内障手術の方が望ましいと考える。

緑内障ガイドライン第3版では，隅角閉塞を上述の機序で分類しているほかに，発症速度により，急性型と慢性型に分類している。急性型は隅角の広範な閉塞により短時間に眼圧が上昇し，慢性型は隅角の閉塞が徐々にあるいは間欠的に生ずるために眼圧

上昇が軽微かつ緩徐なものである。急性型はいわゆる急性緑内障発作に代表される。急性緑内障発作は，急激な眼圧上昇に加え，眼痛，嘔気といった自覚症状も強いため，至急，瞳孔ブロックを解除する必要がある。従来はレーザー虹彩切開術（laser iridotomy 以下 LI）や周辺虹彩切除術（peripheral iridotomy 以下 PI）が第一選択であったが，LI後水疱性角膜症が知られるようになったことや，LIやPIでは眼圧下降が得られないことも多い。そこで，最近では，瞳孔ブロックの解除を目的として白内障手術を行うことも多くなっている（**図3～6**）。辻ら[8]は，9例10眼の急性緑内障発作の症例に対してGSL併用白内障手術を行い，1回の手術で良好な眼圧コントロールを得られ，術前の平均隅角周辺虹彩癒着範囲は89％であったと報告している。瞳孔ブロックの期間の長い症例などでは，周辺虹彩前癒着が進行している例も多くあり，また，GSLに伴う重篤な合併症の報告もほとんどなく，機器の進歩により特別に難易度の高い手術ではなくなってきている。これらのことから，緑内障発作に対しても，GSL単独ではなく，GSL併用白内障手術が望ましいと考える。

3. 最後に

緑内障手術時に同時に白内障手術を実施するか否かはいまだに議論の分かれるところではある。最近の手術の進歩は著しく，白内障手術は極小切開白内障手術が行われることが多くなっている。緑内障手術もチューブシャント手術が日本でも行われるようになり，緑内障ガイドライン第3版でも初めて明記された。今後の緑内障手術においてはこれらの手術の進歩に合わせて，高齢化社会などの患者背景も相まって白内障手術が併用されることが多くなると考える。

文　献

1) El-Sayyad FF, Helal MH, Khalil MM, et al：Phacotrabeculectomy versus two-stage operation：A matched study. Ophthalmic Surg Lasers, **30**：260-265, 1999.
2) 黒田真一郎：緑内障白内障同時手術－線維柱帯切除術（LECT），線維柱帯切開術（LOT）－. IOL&RS, **20**：101-105, 2006.
3) 狩野　廉，桑山泰明：濾過胞眼に対する角膜切開超音波白内障手術の影響，あたらしい眼科，**17**：1135-1138, 2000.
4) Aung T, Tow SL, Yap EY, et al：Trabeculectomy for acute primary angle closure. Ophthalmology, **107**：1298-1302, 2000.
5) 鈴木三保子，狩野　廉，桑山泰明：原発閉塞隅角緑内障に対するトラベクレクトミー白内障同時手術の成績．眼紀，**56**：270-273, 2005.
6) 松村美代，溝口尚則，黒田真一郎，他：PEA＋IOLとトラベクロトミーの手術順と術後眼圧．眼科手術，**10**：599-601, 1997.
7) 河野眞一郎：白内障＋緑内障同時手術：その効果と問題点－PEA＋IOL＋隅角癒着解離術－．眼科手術，**10**：137-141, 1997.
8) 辻　隆宏，小堀　朗，唐松　純，他：閉塞隅角による急性緑内障発作に対する白内障手術と隅角癒着解離術の成績．臨眼，**63**：87-92, 2009.

（**別刷請求先**）日野智之　〒602-0841　京都市上京区川原町通広小路上ル梶井町465　京都府立医科大学眼科学教室

Tokuda et al. BMC Research Notes 2014, 7:780
http://www.biomedcentral.com/1756-0500/7/780

BMC Research Notes

RESEARCH ARTICLE Open Access

The defect of SFRP2 modulates an influx of extracellular calcium in B lymphocytes

Yuichi Tokuda†, Masami Tanaka†, Tomohito Yagi† and Kei Tashiro*

Abstract

Background: In the Wnt pathway, the secreted frizzled-related protein 2 (SFRP2) is thought to act as one of the several competitive inhibitors of Wnt. However, the precise role of SFRP2 is still poorly understood especially in B lymphocytes. Here, we investigated the function of SFRP2, comparing the SFRP2 defective as well as normal B lymphocytes in mice.

Results: We demonstrated that calcium influx from extracellular to intracellular space in splenic B cells was clearly affected by the defect of SFRP2. In addition, the phosphorylation of phospholipase Cγ2 was observed to be reduced in SFRP2 defective splenic B cells with B cell receptor stimulation.

Conclusions: SFRP2 is suggested to modulate the influx from extracellular calcium in the B cell receptor signaling pathway.

Keywords: SFRP2, PLCγ2, Calcium influx, B cell receptor signaling

Background

The Wnt pathway is one of the important signal mechanisms related to cell differentiation in embryogenesis, hematopoiesis, and carcinogenesis [1]. It is mainly divided into three categories as Wnt/β-catenin, Wnt/planar cell polarity, and Wnt/calcium pathway [2-5]. In particular, the Wnt/β-catenin pathway, which also termed as "canonical pathway", has been investigated extensively and well understood, comparing to other pathways termed as "noncanonical pathway" [6,7].

The Wnt protein is one of the extracellular ligands binding to the family of Frizzled receptors associated with several receptor-related proteins. Also, the Wnt pathways are regulated with activators or inhibitors [8]. Especially, the secreted frizzled-related protein 2 (SFRP2) (also known as SDF5 [9]) is a competitive inhibitor to act as antagonist of the Wnt pathway [10,11].

During embryogenesis, where Wnt signaling is involved, the defect of *Sfrp2* causes brachysyndactyly in mice [12]. Our previous research also showed that the dysfunction of SFRP2 protein yields a phenotype of preaxial synpolydactyly and syndactyly [13]. Moreover, SFRP2 has reported to be hypermethylated in the prostate cancer [14], gastric cancer [15], and colorectal cancer [16], and to suppress bone formation in multiple myeloma cells [17]. On the other hand, the Wnt is known to maintain hematopoietic stem cells (HSCs) in the bone marrow (BM) niche under the both canonical [18] and noncanonical pathways [6], and various Wnt antagonists such as SFRP2 are suggested to play a role in the regulation of HSCs. In the Wnt pathways of hematopoiesis, SFRP2 as secreted protein is suggested to inhibit the Wnt pathway and maintain the quiescent of HSCs in mice [19]. SFRP2 is also known to be expressed in osteoblasts in BM and related to the proliferation of HSCs [20]. However, the function of SFRP2 on immune system is still unclear, especially in the calcium signaling of B lymphocytes.

Here, we demonstrated that SFRP2 modulates the calcium signal transduction associated with activation cascade in downstream of B cell receptor (BCR) signaling pathway.

Methods

Mice

Mice of wild-type (*Sfrp2*$^{+/+}$) C57BL/6 and of *Sfrp2*-defective strains (*Sfrp2*$^{-/-}$) were bred under the specific pathogen-free (SPF) conditions as described in our previous study [13]. In this study, all mice were examined at 10-12 weeks of age. Reproducibility of data was confirmed by repeating each experiment at least more

* Correspondence: tashiro@koto.kpu-m.ac.jp
†Equal contributors
Department of Genomic Medical Sciences, Kyoto Prefectural University of Medicine, 465 kajii-cho, Kawaramachi-Hirokoji, Kamigyo-ku, Kyoto 602-8566, Japan

than three pairs of *Sfrp2*$^{+/+}$ and *Sfrp2*$^{-/-}$. All procedures in mouse experiments followed the guidelines and were approved by the Kyoto Prefectural University of Medicine Animal Care and Use Committee.

Cell preparation

The cell suspensions were obtained from the BM and spleen samples. After the elimination of red blood cells, the cells in the BM or spleen were suspended in phosphate buffered saline (PBS) with 3% fetal bovine serum. For the western blotting, the splenic B cells were purified by negative isolation using Dynabeads® Mouse CD43 (Untouched™ B Cells) (Invitrogen, Carlsbad, CA, USA) according to the manufacturer's protocol.

Cell differentiation analysis

BM cells were stained by the monoclonal antibodies against the surface markers as follows: FITC-conjugated anti-IgM (II/41), anti-CD43 (S7) and APC-conjugated anti-CD45R/B220 (RA3-6B2; anti-B220). Splenocytes were similarly stained by the monoclonal antibodies as follows: FITC-conjugated anti-CD21/CD35 (7G6), PE-Cy7-conjugated anti-IgM (R6–60.2), anti-B220 antibody (BD Pharmingen, San Diego, CA, USA) and PE-conjugated anti-CD23 (B3B4) antibody (eBioscience, San Diego, CA, USA). All flow cytometry (FACS) experiments were performed by BD FACS Canto II and BD FACSDiva software version 6.1.3 (BD Biosciences, San Jose, CA, USA) according to the manufacturer's protocol. The analysis was performed using the FlowJo software (Tree Star, San Carlos, CA, USA).

Calcium influx analysis

Cell suspensions of splenocytes were incubated at 37°C for 45 min with Fluo 4-AM (Fluo4; Dojindo, Kumamoto, Japan) and Fura Red™ AM (Fura Red; Invitrogen), which final concentrations were 3 μM and 6 μM, respectively. After stained with anti-B220, the cells were resuspended in calcium-free Hank's balanced salt solution (HBSS/Ca^-). Intracellular calcium levels were assessed by the ratio of the intensities of Fluo4/Fura Red [21], which the ratios were averaged for every 10 sec. In the experiments, anti-mouse IgM F(ab')$_2$ fragments (anti-IgM; final concentration 10 μg/ml in HBSS/Ca^-, Jackson Immunoresearch, West Grove, PA, USA) and ethylene glycol bis(2-aminoethyl)-N,N,N',N'-tetraacetic acid (EGTA; final concentration 0.5 mM in HBSS/Ca^-), and calcium (Ca; $CaCl_2$ final concentration 1.26 mM in HBSS/Ca^-) were applied. These experiments were replicated at least three times.

Endoplasmic reticulum (ER) analysis

The splenocytes were incubated at 37°C in 5% CO_2 for 45 min in PBS (Mg^+, Ca^+) and 1 μM ER-Tracker™ Green dye (glibenclamide BODIPY® FL, ER-Tracker; Molecular Probes, Invitrogen) to evaluate the ER abundance [22]. After staining with anti-B220 for 10 min, the cells were resuspended in PBS (Mg^+, Ca^+) for FACS analysis.

Reverse Transcription Polymerase Chain Reaction (RT-PCR)

RT-PCR experiments were performed with Multiple Tissue cDNA (MTC) panels of Mouse (Clontech Laboratories, CA, USA) and *Sfrp2*$^{+/+}$ and *Sfrp2*$^{-/-}$ samples, which were from only *Sfrp2*$^{+/+}$ and both mouse for SFRP2 and β-catenin tests, respectively. The cDNAs from *Sfrp2*$^{+/+}$ and *Sfrp2*$^{-/-}$ mouse samples were synthesized in 20 μl products with 200 ng total RNA from splenic B and BM cells and Super Script II (Invitrogen) according to the manufacturer's protocol. In the PCR process, each cDNA in appropriate mixture was amplified with each specific primer pair, and their details were described in Additional files 1 and 2.

Protein phosphorylation assay by FACS

The phosphorylation assay of proteins was measured by FACS with BD™ Phosflow technology (BD Biosciences) according to the manufacturer's instructions. The stimulations for splenic B cells were examined by anti-IgM antibody (final concentration 10 μg/ml; Jackson Immuno research) or lipopolysaccharide (LPS, final concentration 20 μg/ml; Sigma-Aldrich, San Francisco, CA, USA) in time course of 0, 5, 10, and 15 min. In the case of IgM stimulation, the antibody set of Alexa Fluor® 488 Mouse ERK1/2 (pT202/pY204) (Erk1/2) and PE Mouse anti-Syk (pY348) (Syk) was applied to detect the phosphorylated proteins. In the case of LPS stimulation, Erk1/2 and PE Mouse p38 MAPK (pT180/pY182) (P38) (BD™ Phosflow, BD Biosciences) were examined. These antibodies with anti-B220 were stained for splenic B cells for 30 min in Phosflow experiment process.

Western blotting

The purified splenic B cells were stimulated by anti-IgM (10 μg/ml, Jackson) in HBSS with calcium. The samples were evaluated by antibodies from Antibody Sampler Kits (Cell Signaling Technology, Inc. (CST), Danvers, MA, USA) as follows: anti-phospho-Syk (Tyr525/526), anti-Syk, anti-phospho-Lyn (Tyr507), anti-Lyn, anti-phospho-Btk (Tyr223), anti-Btk, anti-phospho-CD19 (Tyr531), and anti-CD19 from B Cell Signaling Antibody Sampler Kit; anti-phospho-PLCγ2 (Tyr1217), anti-phospho-PLCγ2 (Tyr759), and anti-PLCγ2 antibody from PLCγ Antibody Sampler Kit; anti-phospho-SAPK/JNK (Thr183/Tyr185), and anti-phospho-ATF-2 (Thr71) from Phospho-SAPK/JNK Pathway Antibody Sampler Kit. Moreover, anti-NFAT1, anti-NFAT2, and β-actin antibody (CST) were also applied. These antibodies were detected with anti-rabbit IgG-HRP (CST) as secondary antibody. The signals were detected with the ECL Prime or ECL Plus

Western Blotting Detection System (GE Healthcare UK Ltd., Buckinghamshire, UK) according to the manufacturer's protocol. In addition, the Can Get Signal Immunoreaction Enhancer Solution (Toyobo Co., Ltd, Osaka, Japan) was applied if necessary. The results of western blots were analyzed by ImageJ software (http://imagej.nih.gov/ij/index.html).

Statistical analysis

In order to prepare the FACS data for statistical analysis, Office Excel and Visual C++ (Microsoft, Redmond, Washington, USA) were used. We employed R software (http://www.R-project.org/) to perform the statistical analysis including *t*–test in each FACS data and draw the graphs. In the histograms, error bars indicate standard

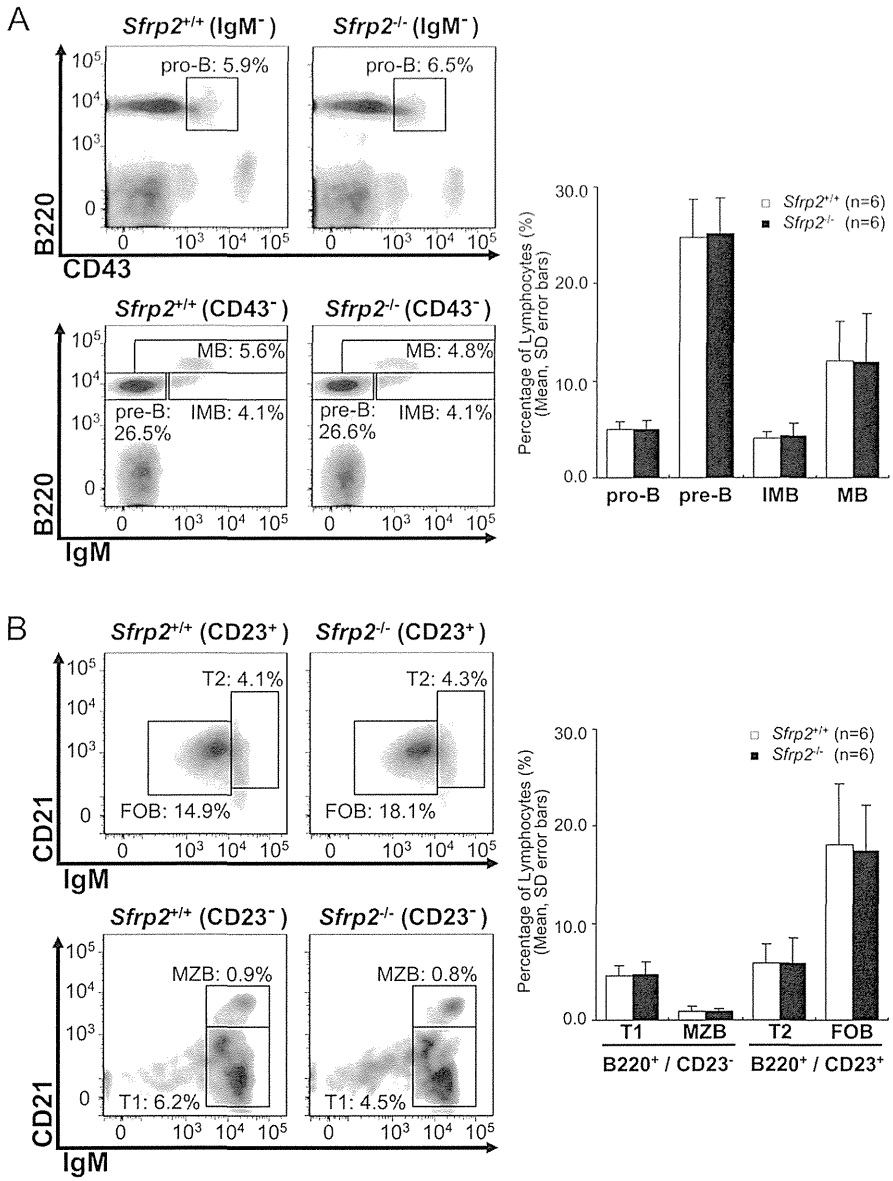

Figure 1 Comparison of BM and splenic B cell differentiation. The cells in the BM or spleen were assessed with each surface marker. The representative FACS plots are demonstrated by FlowJo. **(A)** The results of BM are indicated for B cell differentiation stages of pro-B, pre-B, immature B (IMB), and mature B (MB) cells. The histograms indicate the means and SD of the 6 littermates with same gender pairs for these cell stages. No statistical significant difference between *Sfrp2*$^{+/+}$ and *Sfrp2*$^{-/-}$ in these cell stages was observed by Student's *t*-tests. **(B)** The results of splenic B cells for transitional type 1 (T1), marginal zone B (MZB), transitional type 2 (T2), and follicular B (FOB) cells are indicated. The histograms indicate the means and SD of the 6 gender-matched littermates. In splenic B cells, there was no statistical significant difference between *Sfrp2*$^{+/+}$ and *Sfrp2*$^{-/-}$ by Student's *t*-tests.

deviation with mean. In addition, the R package of "exactRankTests" was used for Wilcoxon tests.

Results

Cell differentiation

In order to evaluate the differences in B cell differentiation, BM and splenic B cells obtained from *Sfrp2*$^{+/+}$ and *Sfrp2*$^{-/-}$ mice were assessed by FACS analysis. No change in B cell differentiation was observed between *Sfrp2*$^{+/+}$ and *Sfrp2*$^{-/-}$ mice by the statistical analysis (Figure 1).

Calcium influx

The differences of calcium signal transduction between *Sfrp2*$^{+/+}$ and *Sfrp2*$^{-/-}$ splenic B cells were evaluated by FACS. No significant difference of intracellular calcium levels was observed with anti-IgM stimulation under the calcium free condition (open arrows in Figure 2). After the addition of extracellular calcium (dotted arrows in Figure 2), intracellular calcium levels rapidly increased because of the influx of extracellular calcium after anti-IgM stimulation. Once reaching the peak, intracellular calcium levels were then gradually decreased with the statistical significant difference between *Sfrp2*$^{+/+}$ and *Sfrp2*$^{-/-}$ splenic B cells (Figure 2A). However, the difference of intracellular calcium levels between *Sfrp2*$^{+/+}$ and *Sfrp2*$^{-/-}$ splenic B cells rapidly disappeared after the removal of extracellular calcium by EGTA (filled arrow in Figure 2B).

ER abundance analysis

ER abundance in splenic B cells was evaluated with ER-Tracker. The results showed that there was no statistical significant difference for ER abundance between the *Sfrp2*$^{+/+}$ and *Sfrp2*$^{-/-}$ splenic B cells (Figure 3).

SFRP2 and β-catenin expression

The expression of SFRP2 studied by RT-PCR was high in BM, but very low in spleen/splenic B cells (Additional file 1). On the other hand, the expression of β-catenin was clearly noted in spleen similar to other tissues, as well as in *Sfrp2*$^{+/+}$ and *Sfrp2*$^{-/-}$ splenocytes (Additional file 2A and B). However, phosphorylated β-catenin was barely detectable in BM or spleen tissues by Western blotting (Additional file 2C).

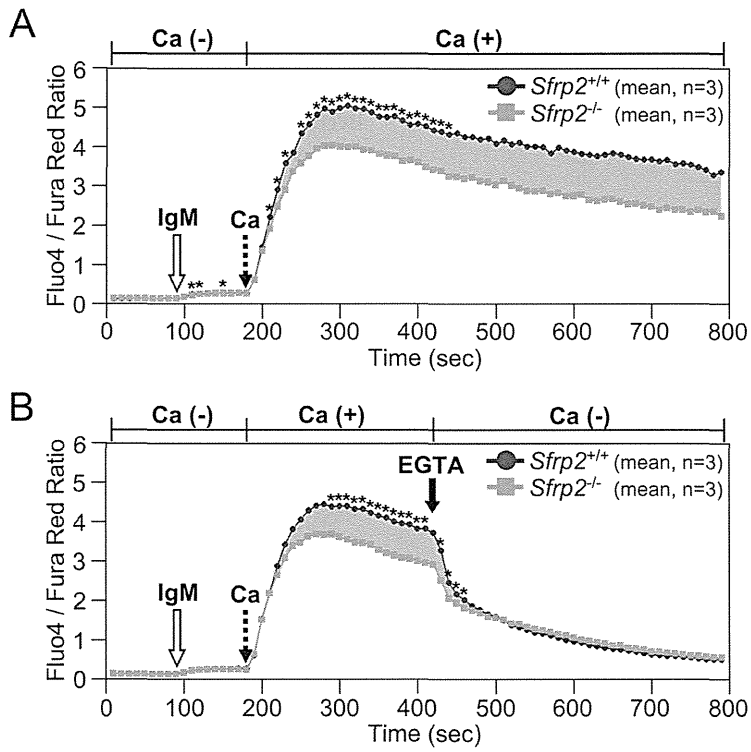

Figure 2 Calcium influx of splenic B cell. The calcium influx in splenic B cells was examined by FACS. The *Sfrp2*$^{+/+}$ and *Sfrp2*$^{-/-}$ splenic B cells were derived from 3 littermates with same gender pair and assessed after gated with anti-B220. The means of 3 replicates are plotted by the blue circles (*Sfrp2*$^{+/+}$) and red squares (*Sfrp2*$^{-/-}$). The black asterisks indicate the statistical significance by paired *t*-test in each time point. Blue shaded regions indicate the differences of intensity ratios between *Sfrp2*$^{+/+}$ and *Sfrp2*$^{-/-}$ splenic B cells. **(A)** After 1.5 min acquisition of signals, the cells were stimulated with anti-IgM (IgM; open arrow). Furthermore, the cells were treated with calcium at 3 min (dotted arrow). **(B)** Following the similar process, the cells were then incubated with EGTA at 7 min (filled arrow).

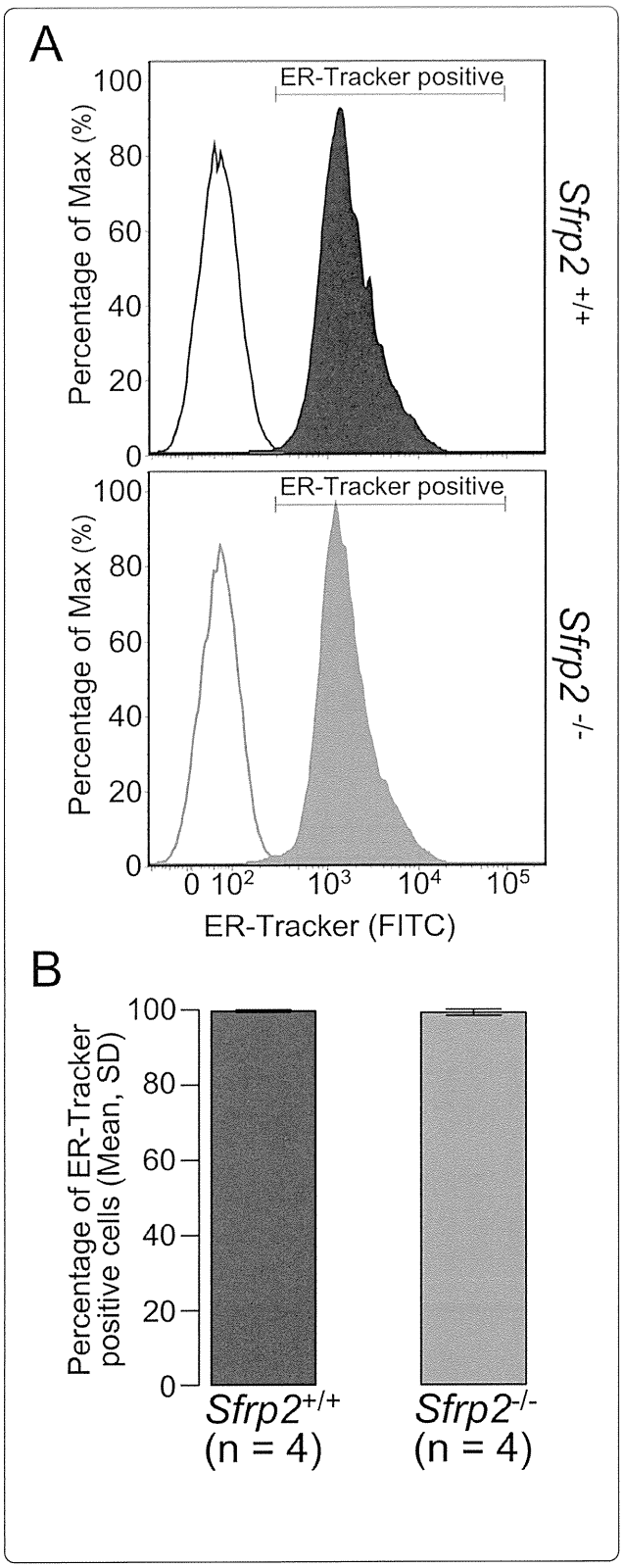

Figure 3 ER abundance of splenic B cell. (A) The representative results of ER abundance in splenic B cells gated with anti-B220 are displayed by using FlowJo. Upper (blue) and lower (red) plots are represented as the percentages of the max of the ER-Tracker signals in splenic B cell of *Sfrp2*$^{+/+}$ and *Sfrp2*$^{-/-}$, respectively. The filled areas indicate ER-Tracker stained B cells and the line areas indicate the intensity of non-stained samples. **(B)** The histograms indicate the means and SD of the 4 littermate pairs for the percentage of ER-Tracker positive cells. No statistical significant difference in ER abundance between *Sfrp2*$^{+/+}$ and *Sfrp2*$^{-/-}$ splenic B cells was observed by Student's *t*-tests.

Western blotting analysis on phosphorylated protein

Before western blots analysis, we first tested each phosphorylation of Erk1/2, P38, and Syk in *Sfrp2*$^{+/+}$ and *Sfrp2*$^{-/-}$ splenic B cells with use of FACS (Additional file 3). Results showed that there was no significant phosphorylation difference between *Sfrp2*$^{+/+}$ and *Sfrp2*$^{-/-}$ when stimulated with either IgM or LPS. Therefore, we examined phosphorylation status of the proteins involved in the BCR signaling pathway with use of western blotting for purified splenic B cells. The purity of splenic B cells was about 98.6% in lymphocytes confirmed by FACS analysis (data not shown).

The phosphorylation of Syk, Lyn, Btk, CD19, and PLCγ2, which is the important downstream effectors of BCR signaling pathway, were assessed comparing with the total amount of each protein. In the western blot analysis, no difference between *Sfrp2*$^{+/+}$ and *Sfrp2*$^{-/-}$ splenic B cells was observed in the time-course experiments after BCR stimulation with anti-IgM (0, 1, 5, 20, and 60 min) (Figure 4A). However, in the Tyr1217 site of PLCγ2, the signals of *Sfrp2*$^{-/-}$ splenic B cells decreased after 5 min stimulation compared with *Sfrp2*$^{+/+}$ samples (Figure 4B). By contrast, no significant difference was observed in the phosphorylation of PLCγ2 at Tyr759 in this study. Accordingly, the defect of *Sfrp2* was considered to affect the phosphorylation of PLCγ2 at Tyr1217 but not Tyr759 in the BCR signaling pathway.

In addition, NFAT1 and NFAT2 were investigated as downstream components of PLCγ2 in the BCR signaling (Figure 4C). Because there was no difference in these proteins between *Sfrp2*$^{+/+}$ and *Sfrp2*$^{-/-}$, the defect of *Sfrp2* was considered not to play a role in the downstream of PLCγ2. Also, in the downstream of calcium signaling cascade related to BCR signaling pathway, no significant difference of phosphorylation in JNK and ATF-2 was found between *Sfrp2*$^{+/+}$ and *Sfrp2*$^{-/-}$ splenic B cells (Figure 4D).

Discussion

In this study, we investigated B lymphocytes in mice affected by the defect of *Sfrp2*, and this defect did not yield the remarkable influence on the early differentiation of B cells (Figure 1). Therefore, we further examined mature B cells in spleen about the influence of the defect of *Sfrp2* in intracellular signal transduction in detail.

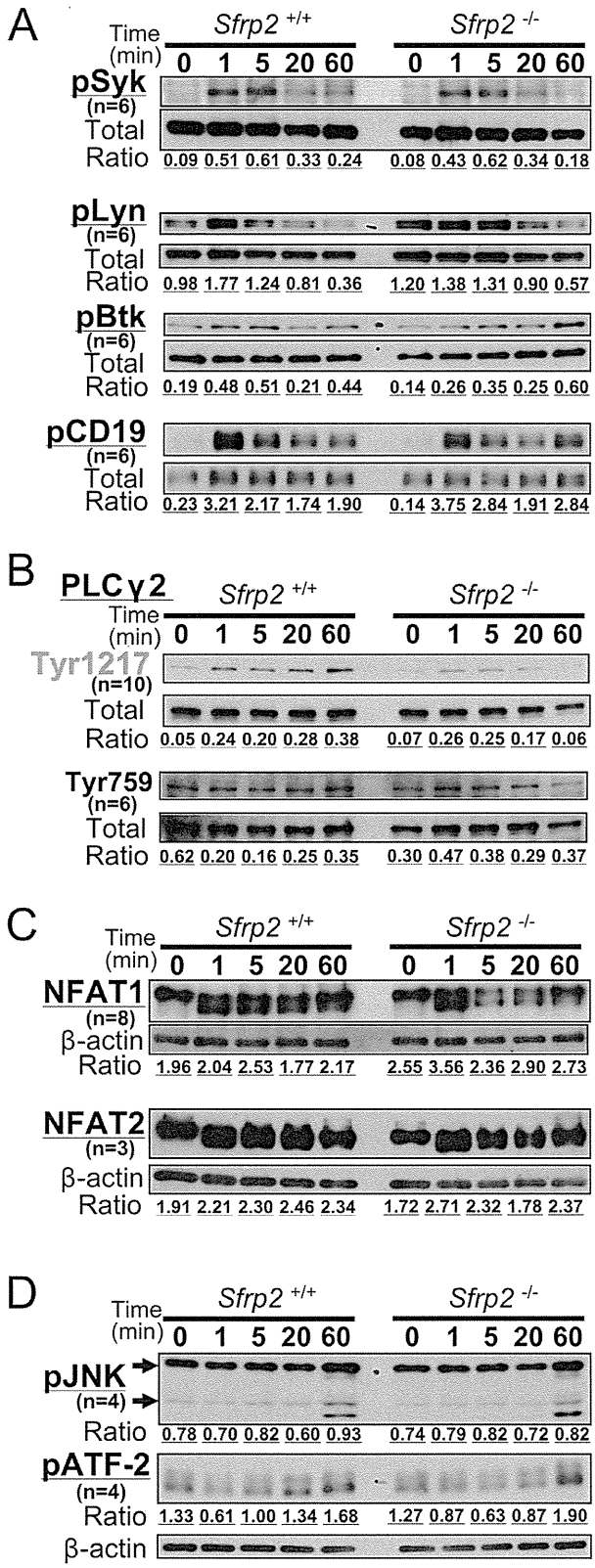

Figure 4 (See legend on next page.)

(See figure on previous page.)
Figure 4 Western blotting results of PLCγ2 splenic B cell. The representative results of western blotting were displayed. Splenic B cells were stimulated with anti-IgM. All experiments were replicated and confirmed three times at least. "n" indicates the number of total tested sample for each protein. **(A)** The phosphorylation of Syk (Tyr525/526; pSyk), Lyn (Tyr507; pLyn), Btk (Tyr223; pBtk), and CD19 (Tyr531; pCD19) sites and **(B)** Tyr1217 and Tyr759 phosphorylation of PLCγ2 were demonstrated with "Total" as the controls, which indicate the amount of each applied protein. **(C)** The expressions of NFAT1 and NFAT2 were indicated with β-actin. **(D)** The phosphorylation of SAPK/JNK (Thr183/Tyr185; pJNK) and ATF-2 (Thr71; pATF-2) were indicated with β-actin. Note that there were two bands for JNK in 54 and 46 kDa due to isoforms as noted by arrows. The ratio of expression level of each sample was calculated by using ImageJ.

The calcium signaling plays a very critical role in the immune system including B cells [23], and so the calcium influx for splenic B cells with *Sfrp2* defect was selectively examined. We showed that the calcium signal transduction by BCR activation was slightly increased in $Sfrp2^{+/+}$ as well as $Sfrp2^{-/-}$ splenic B cells under calcium free condition (open arrows in Figure 2). Moreover, no difference of ER abundance was observed between these B cells (Figure 3). Thus, we could conclude that no significant difference was observed in the intracellular calcium store in both $Sfrp2^{+/+}$and $Sfrp2^{-/-}$ splenic B cells. However, when the calcium was added in the extracellular space (dotted arrows in Figure 2), intracellular calcium levels were rapidly increased in both $Sfrp2^{+/+}$ and $Sfrp2^{-/-}$ splenic B cells due to the influx of extracellular calcium by the BCR stimulation. This was considered to be attributed to the activation of calcium release-activated calcium channel in the plasma membrane triggered by emptying of ER calcium stores under calcium free condition and the first IgM stimulation (open arrows in Figure 2) [23]. Subsequently, intracellular calcium levels gradually decreased and differed significantly between $Sfrp2^{+/+}$ and $Sfrp2^{-/-}$ splenic B cells (Figure 2A). By contrast, intracellular calcium levels were rapidly decreased to the same levels in both splenic B cells after EGTA addition (Figure 2B). Therefore, this phenomenon was observed as a result of the difference of the calcium influx from extracellular to intracellular space between $Sfrp2^{+/+}$ and $Sfrp2^{-/-}$ splenic B cells.

This calcium influx phenomenon is known to be associated with the activation of several proteins involved in the regulation of cell homeostasis. Specifically, protein tyrosine kinases such as Syk and Lyn are initially activated in response to BCR stimulation, which leads to the activation of Btk and CD19. PLCγ2 is then activated by Btk, and cleaves phosphatidylinositol-bisphosphate (PIP_2) into diacylglycerol and inositol (1, 4, 5)-trisphosphate (IP_3) by hydrolysis. Subsequently, IP_3 induced calcium release from intracellular ER calcium stores by binding to the IP_3 receptor. The catalytic hydrolysis of PIP_2 is suggested to require the phosphorylation of Tyr759 in PLCγ2 [24,25]. Moreover, the role of Tyr759 phosphorylation is considered to be different from that of Tyr1217 in PLCγ2 according to the types of cells or stimulations [26]. Our results clearly showed that the defect of *Sfrp2* does not affect the phosphorylation of Syk, Lyn, Btk, and CD19, but reduces the phosphorylation of PLCγ2 at Tyr1217, whereas Tyr759 phosphorylation remained unaffected (Figure 4B). This result may indicate that the *Sfrp2* participates in not pivotally regulating the catalytic hydrolysis of PIP_2 but modulating the calcium signal transduction.

It was unknown if the effect of these defective *Sfrp2* on PLCγ2 is correlated with other abnormal mechanisms in the canonical and/or non-canonical pathways. First, since SFRP2 is not expressed in the hematopoietic cells, especially in splenic B cells compared to BM cells in $Sfrp2^{+/+}$ mice (Additional file 1), exogenous SFRP2 provided from other tissues may contribute to the calcium signaling in the splenic B cell. Moreover, since β-catenin is rarely detectable as protein levels in these splenic B cells (Additional file 2), exogenous SFRP2 may act on the calcium signaling through non-canonical pathway. However, NFAT1, NFAT2, JNK, and ATF-2, which are considered as members of a cascade in downstream of non-canonical signaling pathway, were found not to play a significant role in the $Sfrp2^{-/-}$ splenic B cells (Figure 4C and D). Taken together, the dysregulation of calcium signaling in the $Sfrp2^{-/-}$ splenic B cells occurs under BCR stimulation and is likely to be correlated with unknown common underlying signal pathway(s) of both BCR and non-canonical signalings.

As previously reported, the expression of SFRP2 was down-regulated by methylation in cancer [14,15]. Because calcium signaling was reduced by defect of *Sfrp2*, down-regulation of SFRP2 is assumed to impair the calcium signal transduction in each tissue or cell. However the immune dysfunction was not observed in our SFRP2 deficient mice under the SPF condition, it was reported the association between the methylation of SFRP2 and cancer [14-17]. Although further examination is needed, our results might give us the new insights to understand the functions of SFRP2 under the BCR and calcium signal pathway and the mechanisms of several human diseases.

Conclusions

The defect of *Sfrp2* in mice splenic B cells causes the impairment of calcium influx and the activation of PLCγ2 in the BCR signaling pathway. This phenomenon is speculated to be indirectly related to the activations of Wnt pathways.

Additional files

Additional file 1: The RT-PCR results for SFRP2.

Additional file 2: The expression analyses for β-catenin.

Additional file 3: The results of the phosphorylation experiments with splenic B cells.

Competing interests
The authors declare that they have no competing interests.

Authors' contributions
YT performed a part of experiments, analyzed and summarized all resulting data, and drafted the manuscript; MT centrally kept examined mice and participated in all of experiments; TY participated in all of experiments, designed concrete experimental plan, and helped to draft the manuscript; KT designed general experimental plan and helped to draft the manuscript; All the authors read and approved the final manuscript.

Acknowledgements
We thank T. Ichikawa for excellent secretarial assistance and Dr. S. Imashuku for suggestion and reviewing the manuscript. This work was supported by a Grant-in-Aid for Scientific Research (C: 23590368 to TY) from the Ministry of Education, Culture, Sports, Science and Technology of Japan.

Received: 16 October 2013 Accepted: 24 October 2014
Published: 4 November 2014

References
1. Miller JR: **The Wnts.** *Genome Biol* 2002, **3**:REVIEWS3001.
2. Huelsken J, Behrens J: **The Wnt signalling pathway.** *J Cell Sci* 2002, **115**:3977–3978.
3. Reya T, Clevers H: **Wnt signalling in stem cells and cancer.** *Nature* 2005, **434**:843–850.
4. Suda T, Arai F: **Wnt signaling in the niche.** *Cell* 2008, **132**:729–730.
5. Rao TP, Kuhl M: **An updated overview on Wnt signaling pathways: a prelude for more.** *Circ Res* 2010, **106**:1798–1806.
6. Sugimura R, He XC, Venkatraman A, Arai F, Box A, Semerad C, Haug JS, Peng L, Zhong XB, Suda T, Li L: **Noncanonical Wnt signaling maintains hematopoietic stem cells in the niche.** *Cell* 2012, **150**:351–365.
7. Sugimura R, Li L: **Noncanonical Wnt signaling in vertebrate development, stem cells, and diseases.** *Birth Defects Res C Embryo Today* 2010, **90**:243–256.
8. Cruciat CM, Niehrs C: **Secreted and transmembrane wnt inhibitors and activators.** *Cold Spring Harb Perspect Biol* 2013, **5**:a015081.
9. Shirozu M, Tada H, Tashiro K, Nakamura T, Lopez ND, Nazarea M, Hamada T, Sato T, Nakano T, Honjo T: **Characterization of novel secreted and membrane proteins isolated by the signal sequence trap method.** *Genomics* 1996, **37**:273–280.
10. Satoh W, Matsuyama M, Takemura H, Aizawa S, Shimono A: **Sfrp1, Sfrp2, and Sfrp5 regulate the Wnt/beta-catenin and the planar cell polarity pathways during early trunk formation in mouse.** *Genesis* 2008, **46**:92–103.
11. Mii Y, Taira M: **Secreted Wnt "inhibitors" are not just inhibitors: regulation of extracellular Wnt by secreted Frizzled-related proteins.** *Dev Growth Differ* 2011, **53**:911–923.
12. Morello R, Bertin TK, Schlaubitz S, Shaw CA, Kakuru S, Munivez E, Hermanns P, Chen Y, Zabel B, Lee B: **Brachy-syndactyly caused by loss of Sfrp2 function.** *J Cell Physiol* 2008, **217**:127–137.
13. Ikegawa M, Han H, Okamoto A, Matsui R, Tanaka M, Omi N, Miyamae M, Toguchida J, Tashiro K: **Syndactyly and preaxial synpolydactyly in the single Sfrp2 deleted mutant mice.** *Dev Dyn* 2008, **237**:2506–2517.
14. Perry AS, O'Hurley G, Raheem OA, Brennan K, Wong S, O'Grady A, Kennedy AM, Marignol L, Murphy TM, Sullivan L, Barrett C, Loftus B, Thornhill J, Hewitt SM, Lawler M, Kay E, Lynch T, Hollywood D: **Gene expression and epigenetic discovery screen reveal methylation of SFRP2 in prostate cancer.** *Int J Cancer* 2013, **132**:1771–1780.
15. Cheng YY, Yu J, Wong YP, Man EP, To KF, Jin VX, Li J, Tao Q, Sung JJ, Chan FK, Leung WK: **Frequent epigenetic inactivation of secreted frizzled-related protein 2 (SFRP2) by promoter methylation in human gastric cancer.** *Br J Cancer* 2007, **97**:895–901.
16. Huang Z, Li L, Wang J: **Hypermethylation of SFRP2 as a potential marker for stool-based detection of colorectal cancer and precancerous lesions.** *Dig Dis Sci* 2007, **52**:2287–2291.
17. Oshima T, Abe M, Asano J, Hara T, Kitazoe K, Sekimoto E, Tanaka Y, Shibata H, Hashimoto T, Ozaki S, Kido S, Inoue D, Matsumoto T: **Myeloma cells suppress bone formation by secreting a soluble Wnt inhibitor, sFRP-2.** *Blood* 2005, **106**:3160–3165.
18. Fleming HE, Janzen V, Lo Celso C, Guo J, Leahy KM, Kronenberg HM, Scadden DT: **Wnt signaling in the niche enforces hematopoietic stem cell quiescence and is necessary to preserve self-renewal in vivo.** *Cell Stem Cell* 2008, **2**:274–283.
19. Cain CJ, Manilay JO: **Hematopoietic stem cell fate decisions are regulated by Wnt antagonists: comparisons and current controversies.** *Exp Hematol* 2013, **41**:3–16.
20. Nakajima H, Ito M, Morikawa Y, Komori T, Fukuchi Y, Shibata F, Okamoto S, Kitamura T: **Wnt modulators, SFRP-1, and SFRP-2 are expressed in osteoblasts and differentially regulate hematopoietic stem cells.** *Biochem Biophys Res Commun* 2009, **390**:65–70.
21. Novak EJ, Rabinovitch PS: **Improved sensitivity in flow cytometric intracellular ionized calcium measurement using fluo-3/Fura Red fluorescence ratios.** *Cytometry* 1994, **17**:135–141.
22. Aragon IV, Barrington RA, Jackowski S, Mori K, Brewer JW: **The specialized unfolded protein response of B lymphocytes: ATF6alpha-independent development of antibody-secreting B cells.** *Mol Immunol* 2012, **51**:347–355.
23. Baba Y, Kurosaki T: **Impact of Ca2+ signaling on B cell function.** *Trends Immunol* 2011, **32**:589–594.
24. Humphries LA, Dangelmaier C, Sommer K, Kipp K, Kato RM, Griffith N, Bakman I, Turk CW, Daniel JL, Rawlings DJ: **Tec kinases mediate sustained calcium influx via site-specific tyrosine phosphorylation of the phospholipase Cgamma Src homology 2-Src homology 3 linker.** *J Biol Chem* 2004, **279**:37651–37661.
25. Bunney TD, Katan M: **PLC regulation: emerging pictures for molecular mechanisms.** *Trends Biochem Sci* 2011, **36**:88–96.
26. Kim YJ, Sekiya F, Poulin B, Bae YS, Rhee SG: **Mechanism of B-cell receptor-induced phosphorylation and activation of phospholipase C-gamma2.** *Mol Cell Biol* 2004, **24**:9986–9999.

doi:10.1186/1756-0500-7-780
Cite this article as: Tokuda *et al.*: The defect of SFRP2 modulates an influx of extracellular calcium in B lymphocytes. *BMC Research Notes* 2014 **7**:780.

ON G-BI-ISOVARIANT EQUIVALENCE BETWEEN G-REPRESENTATION SPACES

IKUMITSU NAGASAKI AND FUMIHIRO USHITAKI

ABSTRACT. Let G be a compact Lie group. In this paper, we introduce a new equivalent relation between real G-representation spaces, that is, we say that G-representation spaces V and W are G-bi-isovariantly equivalent and write as $V \rightleftharpoons_G W$ if there exist G-isovariant maps $V \to W$ and $W \to V$. We show that G-bi-isovariant equivalence between real G-representations V, W with $V^G = W^G = \{O\}$ implies $\mathrm{Dim}\, V = \mathrm{Dim}\, W$ if G is finite, or $V \cong W$ if G has positive dimension.

1. INTRODUCTION AND MAIN THEOREM

Throughout this paper, all maps are thought to be continuous. Let G be a compact Lie group. Suppose X and Y are G-spaces. Clearly, every G-equivariant map $\varphi : X \to Y$ satisfies $G_x \subset G_{\varphi(x)}$, where G_x denotes the isotropy subgroup of G at x. A G-equivariant map $\varphi : X \to Y$ is called a *G-isovariant map* if $G_x = G_{\varphi(x)}$ holds for all $x \in X$. In other words, φ is a G-isovariant map if $\varphi|_{G(x)}$ is injective, where $G(x)$ denotes the G-orbit through x.

In this article, we will consider G-isovariant maps between real G-representation spaces. Let V and W be real G-representations with the G-fixed point sets V^G and W^G respectively. By using Wassermann's results proved in [6], we can easily show the following result.

Proposition 1.1 (Isovariant Borsuk-Ulam theorem). *Let G be a compact solvable Lie group. If there is a G-isovariant map $\varphi : V \to W$, then the Borsuk-Ulam inequality*

$$\dim V/V^G \leqq \dim W/W^G,$$

that is,

$$\dim V - \dim V^G \leqq \dim W - \dim W^G$$

holds.

Incidently, the reason why Propositon 1.1 is called Isovariant Borsuk-Ulam theorem is what it is originated from the Borsuk-Ulam theorem ([1]):

2000 *Mathematics Subject Classification.* Primary 57S17; Secondary 55M20, 55M35.

Key words and phrases. Borsuk-Ulam theorem; Borsuk-Ulam groups; isovariant maps; bi-isovariant equivalence:transformation groups; finite group action.

Proposition 1.2 (The Borsuk-Ulam theorem). *Let C_2 be a cyclic group of order 2. Assume that C_2 acts on both S^m and S^n antipodally. If there exists a continuous C_2-map $f : S^m \to S^n$, then $m \leqq n$ holds.*

It is unknown whether similar statements as Propositon 1.1 hold for any compact Lie group. The group G is called a Borsuk-Ulam group (BUG) if whenever there is a G-isovariant map $\varphi : V \to W$, then the Borsuk-Ulam inequality

$$\dim V/V^G \leqq \dim W/W^G,$$

that is,

$$\dim V - \dim V^G \leqq \dim W - \dim W^G$$

holds. Wasserman conjectured that all compact Lie groups are BUGs. He gave a sufficient condition called the prime condition for being a BUG. In our previous work [2], we proved that it is not necessary, that is, we showed there are infinitely many finite groups which does not satisfy it. For the proof, we introduced a new sufficient condition called the Möbius condition.

In the present work, we introduce a new aspect. Namely, we give insight to the relationship between V and W when there exists an isovariant map from not only V to W but also W to V without the assumption that G is a BUG.

Definition 1.3. Let G be a compact Lie group. Let V and W be G-representations. We say that V and W are G-bi-isovariantly equivalent and write as $V \rightleftharpoons_G W$ if there exist G-isovariant maps $V \to W$ and $W \to V$.

Clearly G-bi-isovariant equivalence is an equivalent relation, and $V \rightleftharpoons_G W$ implies $V \rightleftharpoons_H W$ for any subgroup H.

Let $\mathcal{S}(G)$ be the set of all subgroup of G, V a real G-representation space. We define the dimension function

$$\mathrm{Dim}\, V : \mathcal{S}(G) \to \mathbb{Z} \quad \text{by} \quad H \mapsto \dim V^H.$$

Then, we have the following theorem :

Theorem 1.4. *Let G be a compact Lie group, and V, W real G-representations such that $V^G = W^G = \{O\}$. Assume $V \rightleftharpoons_G W$. Then, $\mathrm{Dim}\, V = \mathrm{Dim}\, W$, that is, $\dim V^H = \dim W^H$ holds for any $H \in \mathcal{S}(G)$. Moreover, if $\dim G > 0$ and G is connected, then V is isomorphic to W as G-representations.*

This article is constructed as follows. In section 2, we give a proof of our theorem when G is finite. In the last section, we explain that isovariant condition is essential in our result, and generalize our main theorem.

2. Proof of our theorem

In this section we prove our theorem when G is finite. The non finite case is shown by using Traczyk's result ([4]), which will be shown in our upcoming paper.

Let G be a finite group. For any $H \in \mathcal{S}(G)$, it holds that

$$\dim V = \frac{1}{|H|}\sum_{g\in H}\chi_V(1). \quad \dim V^H = \frac{1}{|H|}\sum_{g\in H}\chi_V(g).$$

Hence,

$$\dim W - \dim W^H - (\dim V - \dim V^H) = \frac{1}{|H|}\sum_{g\in H}(\chi_W(1) - \chi_W(g) - \chi_V(1) + \chi_V(g)).$$

Put

$$h(H) = \sum_{g\in H}(\chi_W(1) - \chi_W(g) - \chi_V(1) + \chi_V(g)).$$

Then, by [2] we see that

$$h(H) = \sum_{D\in \mathrm{Cycl}(H)}\Big(\sum_{D\leqq C:\mathrm{cyclic}\leqq H}\mu(D,C)\Big)h(D),$$

where $\mathrm{Cycl}(H)$ denotes the set of all cyclic subgroups of H, and $\mu(\ ,\ )$ is the Möbius function. Since $D \in \mathrm{Cycl}(H)$ is a BUG and $V \rightleftharpoons_G W$, we have

$$\dim V - \dim V^D = \dim W - \dim W^D,$$

that is, $h(D) = 0$ by Proposition 1.1. Thus, we have

$$\dim V - \dim V^H = \dim W - \dim W^H$$

for any subgroup H of G. Since $V^G = W^G = \{O\}$, by choosing G as H, we see that $\dim V$ must be equal to $\dim W$, and consequently $\mathrm{Dim}\, V = \mathrm{Dim}\, W$.

3. Remarks

Our theorem does not hold without the assumption that the maps are isovariant. Waner gave a necessary and sufficient condition for the exixtence of a G-map from $S(V) \to S(W)$ with $V \supset W$, where $S(V)$ and $S(W)$ denote the unit spheres ([5]). By using Waner's criterion, we see the following :

Example 3.1. Let $G = C_{pq}$ a cyclic group of order pq where p and q are distinct prime numbers. For $i = 1, p, q$, let (T_i, ρ_i) be the complex 1-dimensional representation of G such that $\rho_i(g)(z) = \zeta^i z$, where $z \in \mathbb{C}$ and $\zeta = \exp\dfrac{2\pi\sqrt{-1}}{pq}$. Put

$$V = T_1 \oplus T_p \oplus T_q \quad \textit{and} \quad W = T_p \oplus T_q.$$

Then, they satisfy Waner's criterion, thereby, there exist a G-map from $S(V)$ to $S(W)$.

As is stated in Theorem 1.4, if G is finite, $\mathrm{Dim}\, V = \mathrm{Dim}\, W$ holds. Do there exist finite groups such that $V \rightleftharpoons_G W$ imply $V \cong W$? At the last of this article, we give insight to the problem.

Decompose V and W into the direct sums of irreducible representations as

$$V = V_1 \oplus V_2 \oplus \cdots \oplus V_r \quad \text{and} \quad W = W_1 \oplus W_2 \oplus \cdots \oplus W_s.$$

Then, according to tom Dieck's book [3], $\mathrm{Dim}\, V = \mathrm{Dim}\, W$ if and only if $r = s$ and for each i, V_i is Galois conjugate to some $W_{\sigma(i)}$, where σ is a permutation of $\{1, 2, \ldots, r\}$, that is, there exists $\psi \in Gal(\mathbb{Q}(\zeta_n)/\mathbb{Q})$ such that $\psi(\chi_{V_i}) = \chi_{W_{\sigma(i)}}$, where $n = \mathrm{LCM}\{\ |g|\ |\ g \in G\}$. Thus, we obtain the following :

Proposition 3.2. *Let G be a finite group, and V, W real G-representations such that $V^G = W^G = \{O\}$. Under the above conditions, if the action of $Gal(\mathbb{Q}(\zeta_n)/\mathbb{Q})$ is trivial, $V \rightleftharpoons_G W$ implies $V \cong W$.*

As a corollary, we have :

Corollary 3.3. *Let G be a finite group. Let V and W be real G-representation spaces such that $V^G = W^G = \{O\}$. Assume $V \rightleftharpoons_G W$. Then, if $\chi_V \in \mathbb{Q}$, then $V \cong W$.*

We can illustrate some examples.

Example 3.4. Let G be one of the following groups. Let V and W be real G-representation spaces such that $V^G = W^G = \{O\}$. Then, the characters of all real G-representations take the value in $\mathbb{Q}$. Therefore, $V \rightleftharpoons_G W$ implies $V \cong W$.

- $\mathfrak{S}_n$: the symmetric group of degree n with $n \in \mathbb{N}$.
- C_n : the cyclic group of order n with $n = 2, 3, 4, 6$.
- $C_2^k \times C_3^\ell$: the direct product of C_2's and C_3's, where $k, \ell \geqq 0$.
- C_4^k : the direct product of C_4's, where $k \geqq 1$.
- Q_8^k : the direct product of the quaternion group Q_8's, where $k \geqq 1$.
- D_4^k : the direct product of the diheadral group D_4's, where $k \geqq 1$.